

Mapping the Wigner distribution function of the Morse oscillator
into a semi-classical distribution function

G. W. Bund¹ * and M. C. Tijero^{1,2} †

¹ *Instituto de Física Teórica*

Universidade Estadual Paulista

Rua Pamplona, 145

01405-900– São Paulo, SP

Brazil

² *Pontifícia Universidade Católica de São Paulo*

Rua Marquês de Paranaguá, 111

01303-000– São Paulo, SP

Brazil

*electronic address: bund@ift.unesp.br

†electronic address: maria@ift.unesp.br

Abstract

The mapping of the Wigner distribution function (WDF) for a given bound-state onto a semiclassical distribution function (SDF) satisfying the Liouville equation introduced previously by us is applied to the ground state of the Morse oscillator. Here we give results showing that the SDF gets closer to the corresponding WDF as the number of levels of the Morse oscillator increases. We find that for a Morse oscillator with one level only, the agreement between the WDF and the mapped SDF is very poor but for a Morse oscillator of ten levels it becomes satisfactory.

PACS numbers: 03.65.-w; 03.65.Sq

I. INTRODUCTION

The Wigner description in phase-space [1] provides a tool for comparing quantum and classical dynamics [2]. In a previous paper [3] we introduced a mapping relating the Wigner distribution function (WDF) corresponding to a given wave function, solution of the Schrödinger equation to a semiclassical distribution function (SDF) satisfying the classical Liouville equation with the same potential. So far this mapping was applied to the ground state of the square well [3], the Pöschl-Teller potential [4] and to a modified harmonic oscillator potential [4].

Here this mapping is extended to the ground state of the unidimensional Morse oscillator. We vary the depth of the potential in order to study the effect of the level density on the mapping.

The Morse oscillator [5] plays an important role in many areas of Physics, because it is a good approximation to diatomic molecular potentials [6]. Today the Morse potential is used in molecular spectroscopy, even for polyatomic molecules [7]. Some authors have used the Morse potential for studying the semiclassical limit of Quantum Mechanics [8].

The unidimensional Morse oscillator in phase-space has been already studied by many authors. The classical motion [9] as well as the quantum representation [6] are well known for this potential.

In Sec. II of this work we summarize the method developed in Ref. [3] for mapping WDF into SDF. In Sec. III we study the Morse oscillator and in Sec. IV we present our results and conclusions.

II. DESCRIPTION OF THE METHOD

In this section we present a short derivation of the method used for the mapping [3]. We start with the quantum Liouville equation for the WDF ρ :

$$\frac{\partial \rho}{\partial t} + \frac{p}{m} \frac{\partial \rho}{\partial q} + \int K(q, p - p') \rho(q, p', t) dp' = 0, \quad (1)$$

where the kernel K is given by

$$K(q, p - p') = \frac{i}{\hbar} \int \frac{dv}{2\pi\hbar} \exp \left[\frac{i}{\hbar} (p - p')v \right] \left[V \left(q - \frac{v}{2} \right) - V \left(q + \frac{v}{2} \right) \right], \quad (2)$$

$V(q)$ being the potential. The corresponding classical Liouville equation may be written similarly

$$\frac{\partial \rho_c}{\partial t} + \frac{p}{m} \frac{\partial \rho_c}{\partial q} + \int K_c(q, p - p') \rho_c(q, p', t) dp' = 0, \quad (3)$$

where

$$K_c(q, p - p') = -\frac{i}{\hbar} \int \frac{dv}{2\pi\hbar} \exp \left[\frac{i}{\hbar} (p - p')v \right] v \frac{\partial V}{\partial q} = -\frac{\partial V}{\partial q} \frac{\partial}{\partial p} \delta(p - p'). \quad (4)$$

We relate solutions ρ and ρ_c of Eqs. (1) and (3) through the integral equation

$$\begin{aligned} \rho(q, p, t) &= \rho_c(q, p, t) - \int_{-\infty}^{\infty} dt' \int dq' dp' G_c(q, p; q', p', t - t') \\ &\quad \times \int dp'' [K(q', p' - p'') - K_c(q', p' - p'')] \rho(q', p'', t'), \end{aligned} \quad (5)$$

where G_c is the retarded Green's function corresponding to the classical Liouville equation (3). In fact Eq. (5) is the defining equation of ρ_c since the WDF ρ is already determined by fixing the wave function solution of the Schrödinger equation. Using the differential equation satisfied by G_c [3] one may easily verify that ρ_c satisfies Eq. (3) provided ρ obeys Eq. (1).

As K_c is the term of lowest order in the expansion of K in a power series of \hbar , $\rho - \rho_c$ contains only corrections of the first and higher order terms in \hbar .

It can be shown from results given in Ref. [3], for a WDF generated from solutions of the Schrödinger equation for which the initial wave function at the time $t = t_0$ is given; assuming $\rho(q, p, t)$ to vanish for $t < t_0$, that ρ_c from Eq. (5) gives simply the classical evolution of $\rho(q, p, t_0)$, that is

$$\rho_c(q, p, t) = \rho(Q(q, p, t_0 - t), P(q, p, t_0 - t), t_0), \quad t \geq t_0. \quad (6)$$

Here $(Q(q, p, \tau), P(q, p, \tau))$ describes the classical trajectory in phase-space of a particle subject to the potential $V(q)$ which at the time $\tau = 0$ occupies the point (q, p) , that is

$$q = Q(q, p, 0), \quad p = P(q, p, 0). \quad (7)$$

In what follows we shall consider mostly the mapping of the time independent WDF $\rho(q, p)$ corresponding to a bound state. In this case, from Eq. (5) one obtains [3] the following prescription for ρ_c ,

$$\rho_c(q, p) = \lim_{\epsilon \rightarrow 0^+} \epsilon \int_{-\infty}^0 d\tau e^{\epsilon\tau} \rho(Q(q, p, \tau), P(q, p, \tau)), \quad (8)$$

which is also time independent. Here $e^{\epsilon\tau}$ is a convergence factor introduced explicitly in the Green's function.

It can be shown [3] that for points (q, p) on closed classical orbits the expression given by Eq. (8) is equivalent to

$$\rho_c(q, p) = \frac{1}{T(q, p)} \int_{-T(q, p)}^0 dt \rho(Q(q, p, t), P(q, p, t)), \quad (9)$$

where $T = T(q, p)$ is the period of the orbit. For open trajectories we have $T \rightarrow \infty$ and as for bound states the integral in Eq. (9) converges, we get $\rho_c = 0$. As it will be discussed further, in the calculation of averages of physical quantities the quantity of interest is rather $T(q, p)\rho_c(q, p)$ which does not vanish for the open trajectories.

We observe here that one may verify directly that the time-independent Liouville equation is obeyed by applying the operator $p\partial/\partial q - (\partial V/\partial q)\partial/\partial p$ on the right hand side of Eq. (8) or (9) and using the fact that $\rho(Q(q, p, -t), P(q, p, -t))$ satisfies the classical Liouville equation (3).

An important property of the stationary SDF is that it is constant along the classical trajectories [3] which can be seen by noticing that for any two points (q, p) and (q', p') on the same path in phase space one has a time interval Δ such that

$$Q(q', p', t) = Q(q, p, t + \Delta), \quad P(q', p', t) = P(q, p, t + \Delta). \quad (10)$$

(Δ is the time which the particle takes to go from the point (q, p) to the point (q', p') in phase space or vice versa). Thus we get

$$\begin{aligned}
\rho_c(q', p') &= \frac{1}{T} \int_{-T}^0 dt \rho(Q(q', p', t), P(q', p', t)) \\
&= \frac{1}{T} \int_{-T}^0 dt \rho(Q(q, p, t + \Delta), P(q, p, t + \Delta)) \\
&= \rho_c(q, p),
\end{aligned} \tag{11}$$

where we used the periodicity of the integrand in the last step.

Let $(Q(E, \nu, t), P(E, \nu, t))$ represent, for t in the interval $-T(E, \nu)/2 \leq t \leq T(E, \nu)/2$ (T may be infinity), the points of a trajectory in phase-space corresponding to energy E and fixed value of ν . Here the discrete parameter ν ($\nu = 1, \dots, \nu_{\max}$) distinguishes between the different trajectories corresponding to the same value of E . By varying E and ν one covers the entire allowed phase space. Thus we may consider the transformation of points (E, ν, t) in the appropriate domains D_ν of the energy-time space onto the points (p, q) of the phase space

$$q = Q(E, \nu, t), \quad p = P(E, \nu, t). \tag{12}$$

Let us define the function

$$R_c(E, \nu) = \int_{-T(E, \nu)/2}^{T(E, \nu)/2} dt \rho(Q(E, \nu, t), P(E, \nu, t)). \tag{13}$$

According to Eq. (9) one has

$$\rho_c(q, p) = \frac{R_c(E(q, p), \nu)}{T(E(q, p), \nu)}, \tag{14}$$

by choosing the value of ν appropriate to the trajectory containing the point (q, p) as follows from Eq. (12). We observe here that the relationship (13) between $\rho(q, p)$ and $R_c(E, \nu)$ is analogous to that between $R(q)$, the probability density in coordinate space and the WDF $\rho(q, p)$ [10]:

$$R(q) = \int \rho(q, p) dp. \tag{15}$$

The average of any Weyl function [10] $\mathcal{O}(q, p)$ corresponding to a certain operator O may be written

$$\langle O \rangle = \int \mathcal{O}(q, p) \rho(q, p) dp dq = \sum_{\nu} \int_{D_{\nu}} o(E, \nu, \tau) r(E, \nu, \tau) dE d\tau, \quad (16)$$

where we introduced the functions

$$o(E, \nu, \tau) = \mathcal{O}(Q(E, \nu, \tau), P(E, \nu, \tau)), \quad (17)$$

$$r(E, \nu, \tau) = \rho(Q(E, \nu, \tau), P(E, \nu, \tau)), \quad (18)$$

and we used the fact that the Jacobian J of the transformation (12) is unity [3]

$$J = \begin{vmatrix} \frac{\partial P}{\partial E} & \frac{\partial Q}{\partial E} \\ \frac{\partial P}{\partial t} & \frac{\partial Q}{\partial t} \end{vmatrix} = \frac{\partial P}{\partial E} \frac{\partial E}{\partial p} + \frac{\partial Q}{\partial E} \frac{\partial E}{\partial q} = 1. \quad (19)$$

In the special case in which the Weyl function \mathcal{O} is a constant of motion depending on (q, p) only through the energy $E(q, p)$, we obtain from (16), (18) and (13)

$$\langle O \rangle = \sum_{\nu} \int_{D_{\nu}} o(E, \nu) r(E, \nu, \tau) dE d\tau = \sum_{\nu} \int o(E, \nu) R_c(E, \nu) dE. \quad (20)$$

In particular the normalization condition for $R_c(E, \nu)$

$$\sum_{\nu} \int R_c(E, \nu) dE = 1, \quad (21)$$

follows from Eq. (20) by taking $\mathcal{O}(q, p) = 1$ since the Wigner function $\rho(q, p)$ is normalized.

As ρ_c is an approximation correct in zeroth order of the expansion in powers of \hbar of the Wigner function ρ , the average

$$\langle O \rangle_c = \int \mathcal{O}(q, p) \rho_c(q, p) dq dp, \quad (22)$$

is also correct in the same order in \hbar . The expression (22) may be also written, by making use of the transformation (12), as

$$\langle O \rangle_c = \sum_{\nu} \int_{D_{\nu}} o(E, \nu, t) \frac{R_c(E, \nu)}{T(E, \nu)} dE dt = \sum_{\nu} \int \bar{o}(E, \nu) R_c(E, \nu) dE, \quad (23)$$

where we used Eqs. (14) and (17) and $\bar{o}(E, \nu)$ denotes the average

$$\bar{o}(E, \nu) = \int_{-T(E, \nu)/2}^{T(E, \nu)/2} o(E, \nu, t) \frac{dt}{T(E, \nu)}. \quad (24)$$

Thus the average $\langle O \rangle_c$ is obtained by replacing $o(E, \nu, t)$ in Eq. (16) by the average (24). If, for fixed E , $o(E, \nu, t)$ depends weakly on t , the average $\langle O \rangle_c$ is expected to be a good approximation.

III. WIGNER DISTRIBUTION FUNCTION FOR THE MORSE POTENTIAL

In 1929 Morse [5] suggested the potential $U_0(1 - e^{-ax})^2$ for studying diatomic molecules. The Schrödinger equation for this potential does not have an exact solution, but for the one dimensional case the problem can be solved analytically [11,12].

In order to obtain the Wigner Distribution Function (WDF) [1]

$$\rho(q, p, t) = (2\pi\hbar)^{-1} \int_{-\infty}^{\infty} dv e^{\frac{i}{\hbar}pv} \psi(q - \frac{1}{2}v, t) \psi^*(q + \frac{1}{2}v, t), \quad (25)$$

where ψ is the solution of the Schrödinger equation, we need the eigenfunctions for the one-dimensional Morse potential

$$\mathcal{V}(x) = D(1 - e^{-ax})^2, \quad (26)$$

a and D being constant parameters. Starting with the Schrödinger equation

$$\left[-\frac{\hbar^2}{2m} \frac{d^2}{dx^2} + D(1 - e^{-ax})^2 \right] \psi_n = \mathcal{E}_n \psi_n, \quad (27)$$

we introduce the dimensionless parameter λ

$$\lambda = \frac{\sqrt{2mD}}{a\hbar}, \quad (28)$$

and the dimensionless coordinate

$$q = ax, \quad (29)$$

obtaining an eigenvalue equation depending only on one parameter

$$\left[-\frac{1}{\lambda^2} \frac{d^2}{dq^2} + (1 - e^{-q})^2 \right] \psi_n = \epsilon_n \psi_n, \quad (30)$$

where

$$\epsilon_n = \frac{\mathcal{E}_n}{D}. \quad (31)$$

This equation is solved most conveniently using the variable

$$\xi = 2\lambda e^{-q}, \quad -\infty < q < \infty. \quad (32)$$

The eigenfunctions and eigenvalues are [6]

$$\psi_n(\xi) = N(n, \lambda) e^{-\frac{\xi}{2}} \xi^{\lambda-n-\frac{1}{2}} L_n^{\lambda-n-\frac{1}{2}}(\xi), \quad (33)$$

$$\epsilon_n = \frac{2}{\lambda} \left(n + \frac{1}{2} \right) \left[1 - \frac{1}{2\lambda} \left(n + \frac{1}{2} \right) \right], \quad (34)$$

where the quantum number n takes the values

$$n = 0, 1, 2, \dots, \left[\lambda - \frac{1}{2} \right]. \quad (35)$$

Here $[\lambda - 1/2]$ denotes the largest integer smaller than $\lambda - 1/2$, L_n^s is the polynomial [6]

$$L_n^s = \sum_{j=0}^n \binom{n+2s}{n-j} \frac{(-\xi)^j}{j!}, \quad (36)$$

and the normalization factor N is given by

$$N(\lambda, n) = \left[\frac{(2\lambda - 2n - 1)\Gamma(n+1)}{\Gamma(2\lambda - n)} \right]^{\frac{1}{2}}, \quad (37)$$

where the normalization condition $\int \psi_n^* \psi_n dq = 1$ is assumed. In Appendix A, Eqs. (33) and (34) are derived.

From Eq. (34) one verifies that, for $\lambda \gg 1$ and $n \ll \lambda$, the energy spectrum of the Morse oscillator is written approximately $\mathcal{E}_n \approx \hbar\omega_0(n + 1/2)$, which is the spectrum of a harmonic oscillator with frequency

$$\omega_0 = \frac{2D}{\hbar\lambda} = a\sqrt{\frac{2D}{m}} = \lambda\hbar\frac{a^2}{m}. \quad (38)$$

As the semiclassical distribution functions ρ_c for the harmonic oscillator coincide with the Wigner functions ρ we expect that if $\lambda \gg 1$ ρ_c does get close to ρ for the low lying levels. Thus it may be appropriate to use, instead of the variable q and its canonical conjugate momentum p , the variables which treat harmonic oscillators on the same footing, namely [6]

$$Q = \left[\frac{m\omega_0}{\hbar} \right]^{\frac{1}{2}} x = \left[\frac{2mD}{a^2\hbar^2\lambda} \right]^{\frac{1}{2}} q = \sqrt{\lambda}q, \quad (39a)$$

$$P = \frac{1}{\sqrt{\lambda}}p. \quad (39b)$$

The coordinate Q and the momentum P have been used in the figures of Sec. IV. We define the dimensionless potential $V(Q)$

$$V(Q) = (\hbar\omega_0)^{-1}\mathcal{V}(x) = \frac{\lambda}{2} \left(1 - e^{-\frac{Q}{\sqrt{\lambda}}}\right)^2, \quad (39c)$$

which is also used in the figures. For the energy levels there we use similarly

$$E_n = (\hbar\omega_0)^{-1}\mathcal{E}_n = \left(n + \frac{1}{2}\right) - \frac{1}{2\lambda} \left(n + \frac{1}{2}\right)^2. \quad (39d)$$

In the special case of our interest, namely the ground state, $n = 0$, the wave function is given by

$$\psi_0(\xi) = \left[\frac{2\lambda - 1}{\Gamma(2\lambda)}\right]^{\frac{1}{2}} \xi^{\lambda - \frac{1}{2}} e^{-\frac{\xi}{2}}. \quad (40)$$

In order to calculate the Wigner function replace ψ by $\psi_n(2\lambda e^{-q})$ into Eq. (25), obtaining

$$\rho_n^{(\lambda)}(q, p) = (2\pi\hbar)^{-1} \int_{-\infty}^{\infty} dv \psi_n(2\lambda e^{[-q + \frac{v}{2}]}) \psi_n^*(2\lambda e^{[-q - \frac{v}{2}]}) e^{\frac{i}{\hbar}pv}. \quad (41)$$

Introducing the new integration variable

$$\tau = e^{\frac{v}{2}}, \quad (42)$$

Eq. (41) becomes

$$\rho_n^{(\lambda)}(q, p) = (\pi\hbar)^{-1} \int_0^{\infty} \psi_n^*\left(\frac{\xi}{\tau}\right) \psi_n(\xi\tau) \tau^{2ip\hbar^{-1}} \frac{d\tau}{\tau}, \quad (43)$$

where ξ is given by Eq. (32). Substituting ψ_n in Eq. (43) by the expression (33) $\rho_n^{(\lambda)}$ becomes [6]

$$\rho_n^{(\lambda)}(q, p) = \left[\frac{\pi\hbar}{2}\right]^{-1} [N(\lambda, n)]^2 \xi^{2\lambda - 2n - 1} \sum_{r=0}^n \sum_{s=0}^n b(\lambda, n, r) b(\lambda, n, s) \xi^{r+s} K_{s-r+2ip\hbar^{-1}}(\xi), \quad (44)$$

where

$$b(\lambda, n, j) = \binom{2\lambda - n - 1}{n - j} \frac{(-1)^j}{j!} \quad (45)$$

and $K_\nu(\xi)$ is defined by [6]

$$K_\nu(\xi) = \frac{1}{2} \int_0^\infty e^{-\frac{\xi}{2}(\tau + \frac{1}{\tau})} \tau^\nu \frac{d\tau}{\tau}, \quad (46)$$

ν being a complex variable. In the particular case in which $n = 0$ we get

$$\rho_0^{(\lambda)}(q, p) = \left(\frac{\pi\hbar}{2}\right)^{-1} \frac{2\lambda - 1}{\Gamma(2\lambda)} \xi^{2\lambda-1} K_{2ip\hbar^{-1}}(\xi). \quad (47)$$

The numerical method we used to calculate the function $K_\nu(\xi)$ will be given in Appendix B.

The symmetries obeyed by the function K_ν are

$$K_{\nu^*}(\xi) = \frac{1}{2} \int_0^\infty e^{-\frac{\xi}{2}(\tau + \frac{1}{\tau})} (\tau^\nu)^* \frac{d\tau}{\tau} = (K_\nu(\xi))^*, \quad (48)$$

$$K_{-\nu}(\xi) = \frac{1}{2} \int_0^\infty e^{-\frac{\xi}{2}(\tau + \frac{1}{\tau})} \tau^{-\nu} \frac{d\tau}{\tau} = K_\nu(\xi), \quad (49)$$

where the last step is obtained by making $\tau \rightarrow \tau^{-1}$. From Eqs.(49) and (48) we get

$$K_{-a+ib} = K_{a+ib}^*. \quad (50)$$

Thus Eq. (44) may be written

$$\rho_n^{(\lambda)}(q, p) = \left[\frac{\pi\hbar}{2}\right]^{-1} [N(\lambda, n)]^2 \xi^{2\lambda-2n-1} \sum_{r=0}^n \sum_{s=0}^n b(\lambda, n, r) b(\lambda, n, s) \xi^{r+s} \text{Re} \left(K_{s-r+2ip\hbar^{-1}}(\xi) \right), \quad (51)$$

showing explicitly that $\rho_n^{(\lambda)}$ is real.

In order to calculate the semiclassical distribution function $\rho_c(q, p)$ given by Eq. (9) or (14), we need the solution of the classical equation of motion

$$m\ddot{x} = -D \frac{d}{dx} (1 - e^{-ax})^2, \quad (52)$$

which has already been obtained exactly [9]. Introducing the coordinate $q = ax$ and the variable θ given by

$$\theta = \omega_0 t, \quad (53)$$

where ω_0 is given by Eq. (38), Eq. (52) becomes

$$2\frac{d^2q}{d\theta^2} = -\frac{d}{dq}(1 - e^{-q})^2. \quad (54)$$

The solution of Eq. (54) for $\epsilon = E/D < 1$, where E is the energy associated with the trajectory, is

$$q(E, t) = \ln \left\{ \frac{1}{1 - \epsilon} \left[1 + \sqrt{\epsilon} \sin \sqrt{1 - \epsilon} (\omega_0 t - \theta_0) \right] \right\}. \quad (55)$$

The canonical momentum associated with q is

$$p = \frac{m\dot{q}}{a^2}, \quad (56)$$

which using Eqs. (55) and (38) gives

$$p(E, t) = \hbar\lambda \frac{\sqrt{\epsilon}\sqrt{1 - \epsilon} \cos[\sqrt{1 - \epsilon}(\omega_0 t - \theta_0)]}{1 + \sqrt{\epsilon} \sin[\sqrt{1 - \epsilon}(\omega_0 t - \theta_0)]}. \quad (57)$$

The period associated with the orbit is

$$T(E) = \frac{2\pi}{\omega_0\sqrt{1 - \epsilon}}. \quad (58)$$

Analising Eq. (55) one obtains that for $E \ll D$ the trajectories are close to those of a harmonic oscillator of frequency ω_0 .

IV. RESULTS

In this section we present the results of our calculations. We calculated the WDF ρ and corresponding SDF ρ_c for the ground state of the Morse oscillator choosing for the parameter λ the values 1,2,4 and 10 corresponding to oscillators with 1,2,4 and 10 levels respectively. In the figures we used throughout the dimensionless coordinates Q and the conjugate momenta P (in units of \hbar) defined by Eqs. (39a) and (39b). In Figs. 1,2,3 and 4 the potentials $V(Q)$ defined by Eq. (39c) are displayed for $\lambda = 1, 2, 4$ and 10 and the energy levels marked. We observe here that the potential given by Eq. (39c) is independent of λ for $Q^2 \ll \lambda$.

Figs. 5,6,7 and 8 reproduce our calculations of the WDF for $\lambda = 1, 2, 4$ and 10 respectively through curves of constant density $\rho(Q, P)$. The value of ρ varies from $\rho \approx 0.3$ to $\rho = 0$ in

the region of phase-space corresponding approximately to the region of the bound classical particles. Then there occur adjacent regions on which ρ alternates from negative to positive values and its magnitude decreases as the region gets farther away from the origin.

In the case $\lambda = 1$ the minimum value of ρ is (in units of \hbar^{-1}) of the order of -10^{-2} , as it can be seen from Fig. 5. This minimum approaches zero as λ increases, which can be observed from Fig. 7 for $\lambda = 4$ where the minimum of ρ is about -10^{-4} .

The maximum of ρ , as it can be verified from Figs. 5—8, moves from the point $(Q, P) = (1.2, 0)$ to $(Q, P) = (0.3, 0)$ as λ increases from 1 to 10 and its value increases slightly as λ increases. Thus the curve for $\rho = 0.3$, present for $\lambda \geq 2$, does not occur for $\lambda = 1$.

Another feature of the WDF is that the curves of constant density ρ become more symmetric with respect to an axis parallel to the P -axis as λ increases, becoming close to the form of an ellipse. This tallies with the fact that for $Q \ll \sqrt{\lambda}$, $V(Q)$ is the potential of a harmonic oscillator.

In Figs. 10,11,12 and 13 we present SDF curves for fixed ρ_c superposed on WDF curves with $\rho = \rho_c$ for comparison. It will be seen that, as λ increases the SDF approximation improves, which means also that the WDF curves of constant ρ become closer to classical trajectories. In Fig. 9 we plot curves of constant ρ_c for the case $\lambda = 1$. For this oscillator our semiclassical approximation is anomalous, as the value of ρ_c increases from $\rho_c = 0.145$ to $\rho_c = 0.179$ as the classical energy E varies from $E = 0$ to $E = 0.26\hbar\omega_0$ but decreases as E increases further. For the other oscillators ρ_c decreases as the energy E increases until reaching the value $\rho_c = 0$. As a consequence for $\lambda = 1$ one has two closed curves with the same ρ_c for $0.145 < \rho_c < 0.179$ whereas for $\lambda \geq 2$, for each ρ_c one has only one such curve. Also for the WDF there is only one closed curve for each ρ from the maximum value of ρ up to the curve $\rho = 0$.

In Fig. 10 we compare the WDF curves of constant ρ with the SDF curves for which $\rho = \rho_c$ in the case $\lambda = 1$. One notices that the discrepancies between both curves are very large. In Figs. 11,12 and 13 we make the same comparison for $\lambda = 2, 4$ and 10 respectively.

One finds that for $\rho < 0.05$ both curves are quite similar but displaced from each other.

This displacement becomes less pronounced as ρ gets closer to 0.05 so that the best agreement between ρ and ρ_c is reached for $\rho \approx 0.05$. Also as λ increases the displacement between both curves decreases, as it can be seen comparing the oscillators $\lambda = 4$ and $\lambda = 10$. For $\rho \gtrsim 0.05$ the curves of fixed ρ_c compared with the curves of fixed ρ contain a certain amount of distortion which becomes less pronounced as λ increases.

Finally we observe that curves with $\rho_c = 0.3$ are absent, the largest values of ρ_c being 0.227, 0.271 and 0.299 respectively for $\lambda = 2, 4$ and 10, values which are reached at the origin of phase-space.

APPENDIX A: EIGENFUNCTIONS AND EIGENVALUES OF THE MORSE POTENTIAL

In this Appendix we solve briefly the eigenvalue equation for the Morse potential (Eq. (30) of Sec. III)

$$\left[\frac{d^2}{dz^2} - \lambda^2(1 - e^{-z})^2 + \lambda^2\epsilon_n \right] \psi_n(z) = 0. \quad (\text{A1})$$

Making the substitution $y = 2\lambda e^{-z}$, Eq. (A1) is written

$$\left[y^2 \frac{d^2}{dy^2} + y \frac{d}{dy} - \lambda^2 \left(1 - \frac{y}{2\lambda}\right)^2 + \lambda^2\epsilon_n \right] \psi_n(y) = 0, \quad (\text{A2})$$

or,

$$\left[\frac{d^2}{dy^2} + \frac{1}{y} \frac{d}{dy} + \frac{(\epsilon_n - 1)\lambda^2}{y^2} + \frac{\lambda}{y} - \frac{1}{4} \right] \psi_n(y) = 0. \quad (\text{A3})$$

Assuming a solution of the form

$$\psi_n(y) = e^{-\frac{y}{2}} y^s u_n(y), \quad (\text{A4})$$

and writing $s^2 = (\epsilon_n - 1)\lambda^2$, from Eq. (A3) we get

$$y u_n'' + (2s + 1 - y) u_n' + \left(\lambda - s - \frac{1}{2}\right) u_n = 0, \quad (\text{A5})$$

where $u'_n = du_n/dy$ and $u''_n = d^2u_n/dy^2$. Making $u_n = \sum_{m=0}^n a_m y^m$, Eq. (A5) may be written as

$$\sum_{m=0}^n [(m+1)(m+2s+1)a_{m+1} + \left(\lambda - s - m - \frac{1}{2}\right) a_m] y^m = 0, \quad (\text{A6})$$

which is the differential equation satisfied by the Laguerre generalized functions. Eq. (A6) is satisfied if

$$a_{m+1} = \frac{s + m - \lambda + \frac{1}{2}}{(m+1)(m+2s+1)} a_m, \quad (\text{A7})$$

which for $m = 0$ is

$$a_1 = \frac{s - \lambda + \frac{1}{2}}{2s+1} a_0. \quad (\text{A8})$$

Since for $m = n$, $a_{m+1} = 0$ and $a_m \neq 0$, Eq. (A7) gives

$$s = \lambda - n - \frac{1}{2}. \quad (\text{A9})$$

Taking into account Eq. (A9) we get

$$-\epsilon_n = -\frac{2}{\lambda} \left(n + \frac{1}{2}\right) + \frac{1}{\lambda^2} \left(n + \frac{1}{2}\right)^2, \quad (\text{A10})$$

and the recurrence relation for the coefficients of the power series in Eq. (A7) becomes

$$a_{m+1} = \frac{m - n}{(m+1)(2\lambda - 2n + m)} a_m. \quad (\text{A11})$$

Choosing

$$a_0 = \frac{(2\lambda - n - 1)!}{n!(2\lambda - 2n - 1)!} N(\lambda, n), \quad (\text{A12})$$

we obtain

$$a_m = \frac{(-1)^m (2\lambda - n - 1)! N(\lambda, n)}{m!(n - m)!(2\lambda - 2n - m - 1)!}, \quad (\text{A13})$$

and we get for ψ_n the expression given by Eq. (33) in Sec. III.

APPENDIX B: NUMERICAL EVALUATION OF THE WIGNER FUNCTION

Here we discuss the numerical calculation of the quantity K_ν defined in Eq. (46) of Sec. III,

$$K_\nu(\xi) = \frac{1}{2} \int_0^\infty e^{-\frac{\xi}{2}(\tau + \frac{1}{\tau})} \tau^\nu \frac{d\tau}{\tau}. \quad (\text{B1})$$

Here ν is complex,

$$\nu = N + 2ik, \quad (\text{B2})$$

where N is an integer and k is the dimensionless momentum p/\hbar and according to Eqs.(32) and (29)

$$\xi = 2\lambda e^{-q}, \quad q = ax. \quad (\text{B3})$$

Making the transformation

$$\tau = e^u, \quad (\text{B4})$$

and considering that only the real part of K_ν enters into the expression (51) for the Wigner function we get from Eq. (B1), substituting also ν according to Eq. (B2),

$$\text{Re}[K_\nu(\xi)] = \frac{1}{2} \int_{-\infty}^{\infty} e^{-\xi \cosh u} e^{uN} \cos(2ku) du. \quad (\text{B5})$$

Let us take initially $N = 0$, which is the only value needed for the ground state of the Morse oscillator. Consider also $k \neq 0$ as the case $k = 0$ is calculated separately. For convenience we introduce the new variable of integration

$$z = 2ku, \quad (\text{B6})$$

and use the fact that the integrand is an even function of u , obtaining from Eq. (B5)

$$\text{Re}[K_\nu(\xi)] = \frac{1}{2k} \int_0^\infty dz e^{-\xi \cosh(\frac{z}{2k})} \cos z. \quad (\text{B7})$$

The integral in Eq. (B7) is of the form

$$I = \int_0^{\infty} f(z) \cos z dz, \quad (\text{B8})$$

where $f(z)$ is a positive decreasing function of z . In order to avoid numerical cancellations arising from the change of sign of $\cos(z)$, we replace this integral by an integral in the interval $[0, \frac{\pi}{2}]$ of a series of functions.

We decompose I as follows

$$I = I_1 + I_2, \quad (\text{B9})$$

where

$$I_1 = \int_0^{\frac{\pi}{2}} f(z) \cos z dz, \quad (\text{B10})$$

and

$$I_2 = \int_{\frac{\pi}{2}}^{\infty} f(z) \cos z dz = - \int_0^{\infty} f(y + \frac{\pi}{2}) \sin y dy, \quad (\text{B11})$$

where we made the substitution $z = y + \frac{\pi}{2}$ in I_2 . The interval of integration of the integral I_2 is divided in the set of intervals $[2\pi s, 2\pi(s+1)]$, $s = 0, 1, \dots$ so that I_2 is written

$$I_2 = - \sum_{s=0}^{\infty} \int_{2\pi s}^{2\pi(s+1)} f(y + \frac{\pi}{2}) \sin y dy. \quad (\text{B12})$$

Making now the substitution

$$z = y - 2\pi s, \quad (\text{B13})$$

for the integral in the interval $[2\pi s, 2\pi(s+1)]$, one obtains for Eq. (B12)

$$I_2 = - \sum_{s=0}^{\infty} \int_0^{2\pi} f(z + (2s + \frac{1}{2})\pi) \sin z dz. \quad (\text{B14})$$

However $\sin z$ changes sign in the interval $[0, 2\pi]$ which leads to cancellation errors if f is slowly varying in the interval. In order to eliminate the oscillation of sign of the integrand we decompose again the integral in the intervals $[0, \pi]$ and $[\pi, 2\pi]$ obtaining

$$I_2 = - \sum_{s=0}^{\infty} \left\{ \int_0^{\pi} \left[f\left(z + \left(2s + \frac{1}{2}\right)\pi\right) - f\left(z + \left(2s + \frac{3}{2}\right)\pi\right) \right] \sin z dz \right\}. \quad (\text{B15})$$

As f is assumed to be monotonically decreasing each integrand in Eq. (B15) is now always positive. As the domain of integration of the integral I_1 is the interval $[0, \frac{\pi}{2}]$ we make the translation $v = z - \frac{\pi}{2}$, obtaining

$$I_2 = - \sum_{s=0}^{\infty} \int_{-\frac{\pi}{2}}^{\frac{\pi}{2}} [f(v + (2s+1)\pi) - f(v + (2s+2)\pi)] \cos v dv. \quad (\text{B16})$$

Making $v \rightarrow -v$ for the contribution from the interval $[-\frac{\pi}{2}, 0]$ in Eq. (B16) and adding the contribution from I_1 one gets finally

$$\begin{aligned} \int_0^{\infty} f(x) \cos x dx &= \int_0^{\frac{\pi}{2}} dx \cos x \{ f(x) - \sum_{s=0}^{\infty} [f((2s+1)\pi - x) + f((2s+1)\pi + x) \\ &\quad - f((2s+2)\pi - x) - f((2s+2)\pi + x)] \}. \end{aligned} \quad (\text{B17})$$

For $f(x)$ monotonic each term of the series contributes with the same sign, however errors may arise from the subtraction of the sum of the series from $f(x)$.

In the general case in which $N \geq 0$ in Eq. (B5), the function $f(z)$ in Eq. (B8) becomes

$$f_N(z) = \frac{1}{2k} e^{-\xi \cosh \frac{z}{2k}} \cosh \left(\frac{Nz}{2k} \right), \quad z \geq 0, \quad N = 0, 1, \dots \quad (\text{B18})$$

The function $f_N(z)$ has M ($M \leq N$) extremes at the real positive points $z_1^{(N)}, z_2^{(N)}, \dots, z_M^{(N)}$, labeled in the order of increasing magnitude. This function decreases monotonically for $z > z_M^{(N)}$ and it may still be useful to apply the decomposition (B17) in order to eliminate errors due to cancellations of contributions of opposite sign from the integrand $f_N(z) \cos z$. In the general case only the sign of the first s_N terms of the series in Eq. (B17) may oscillate, where s_N is given roughly by the smallest integer satisfying $(2s_N + 1)\pi > z_M^{(N)}$. For $s > s_N$ the sign of the terms of the series in Eq. (B17) is always positive.

In fact, one may determine the extremes of $f_N(z)$ by expressing $f_N(z)$ in terms of $\cosh(z/2k)$ and applying the condition $\partial f_N(z)/\partial z = 0$. By making this substitution one gets for Eq. (B18) the expression

$$f_N(z) = \frac{1}{2k} e^{-\xi y} \sum_{j=0}^{[N/2]} A_j (-1)^j y^{N-2j}, \quad y = \cosh\left(\frac{z}{2k}\right), \quad (\text{B19})$$

where $[N/2]$ denotes the largest integer contained in $N/2$ and

$$A_j = \sum_{i=j}^{[N/2]} \binom{N}{2i} \binom{i}{j}. \quad (\text{B20})$$

Thus we get the extrema of $f_N(z)$ as the roots of a polynomial of degree N .

For $N = 1$ the maximum occurs at

$$z_1^{(1)} = 2k \cosh^{-1} \left(\frac{1}{\xi} \right). \quad (\text{B21})$$

For $N = 2$ the maximum will be at

$$z_1^{(2)} = 2k \cosh^{-1} \left(\frac{2}{\xi} + \sqrt{\frac{4}{\xi^2} + 2} \right). \quad (\text{B22})$$

REFERENCES

- [1] E. Wigner, Phys. Rev. **40**, 749 (1932).
- [2] H. W. Lee and M. O. Scully, J. Chem. Phys. **77**(9), 4604 (1982).
- [3] G. W. Bund, J. Phys. **A28** 3709 (1995).
- [4] G. W. Bund and M. C. Tijero, Phys. Rev. A **61**, 052114 (2000).
- [5] P. M. Morse, Phys. Rev. **34**, 57 (1929).
- [6] J. P. Dahl and M. Springborg, J. Chem. Phys. **88**(7), 4535 (1988).
- [7] A. Frank *et al*, Ann. Phys. (N.Y.) **252**, 211 (1996).
- [8] J. P. Dahl, in *Semi-classical Descriptions of Atomic and Nucleon Collisions*, J. Bang and J. de Boer (Eds.) (Elsevier Science Publishers, B.V. 1985).
- [9] W. C. De Marcus, Am. J. Phys. **46**, 733 (1978).
- [10] S. R. Groot and L. G. Suttorp, in *Foundations of Electrodynamics* (Amsterdam: North-Holland, 1972).
- [11] M. M. Nieto and L. M. Simmons Jr. Phys. Rev. A **19**, 438 (1979).
- [12] D. ter Haar, *Problems in Quantum Mechanics*, 3th Edition (Pion, London, 1975).

FIGURES

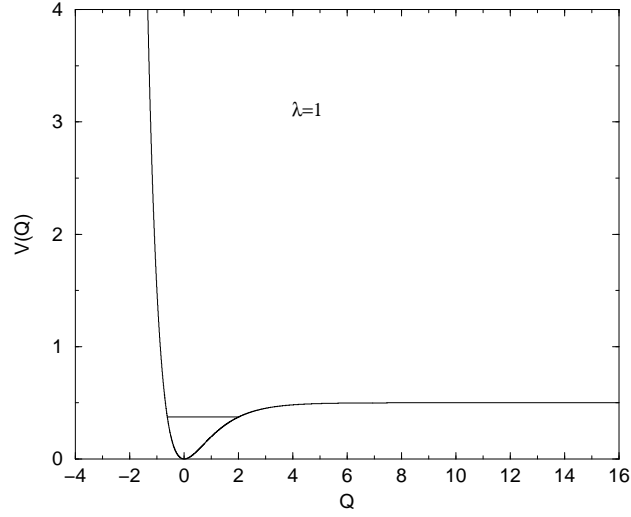


FIG. 1. The Morse potential $V(Q)$ defined by Eq. (39c) and the corresponding bound-state energies E_n given by Eq. (39d), for $\lambda = 1$.

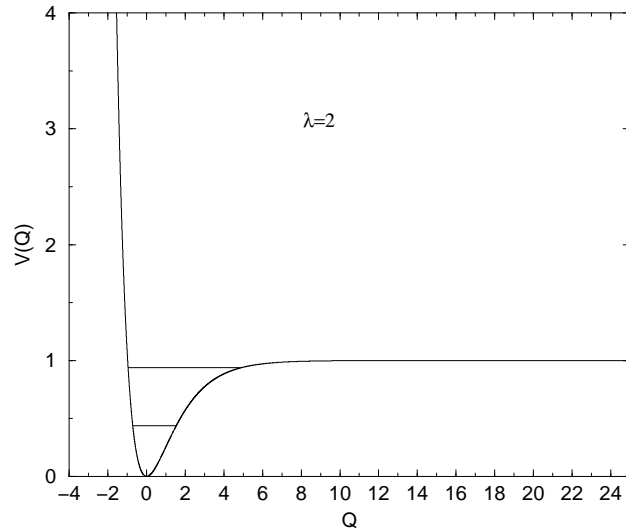


FIG. 2. Same as Fig. 1 for $\lambda = 2$.

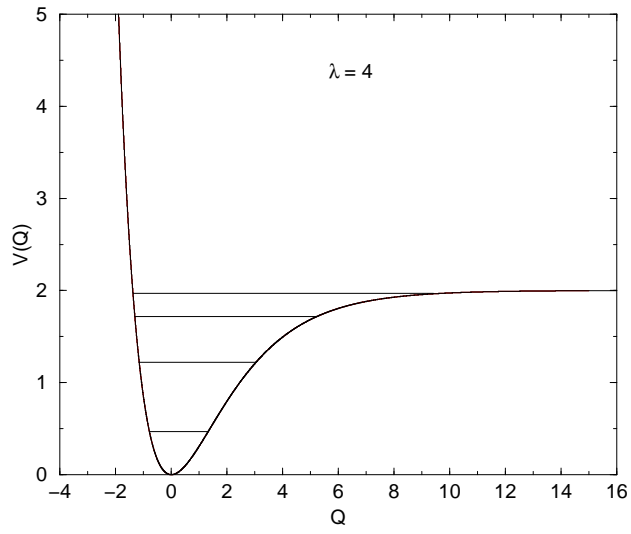


FIG. 3. Same as Fig. 1 for $\lambda = 4$.

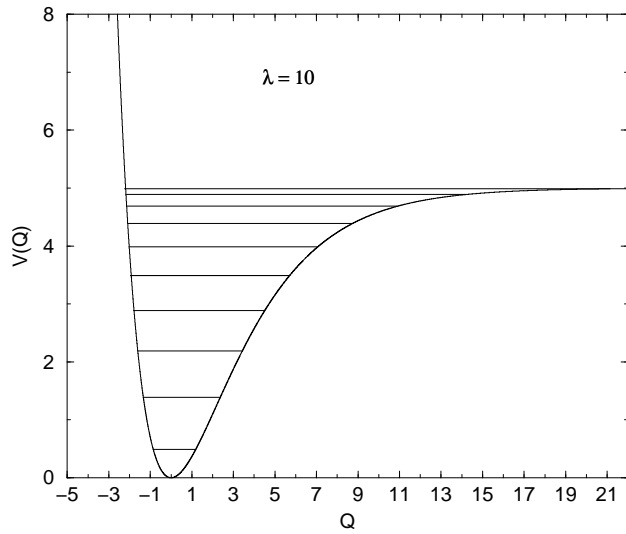


FIG. 4. Same as Fig. 1 for $\lambda = 10$.

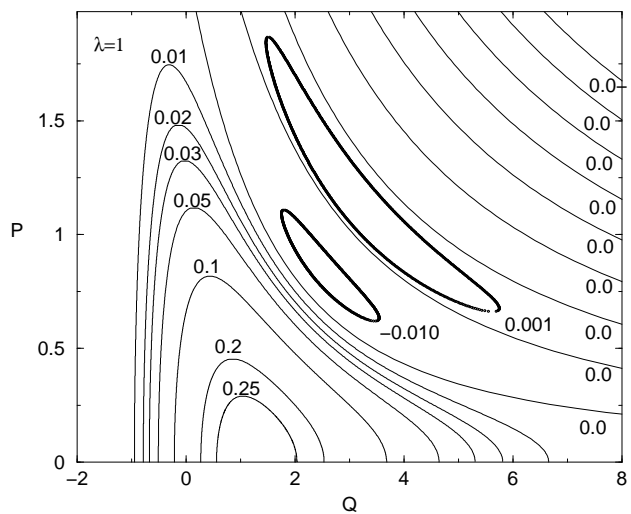


FIG. 5. Curves of constant Wigner distribution function $\rho(Q, P)$ in units of \hbar^{-1} for the ground state of the Morse oscillator with $\lambda = 1$.

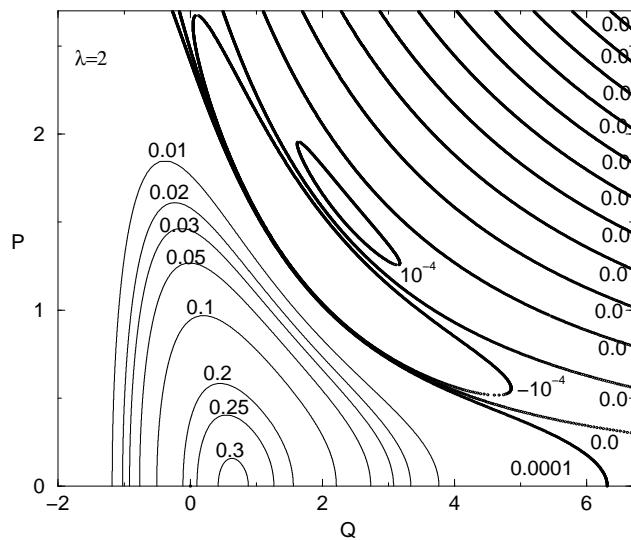


FIG. 6. Same as Fig. 5 for $\lambda = 2$.

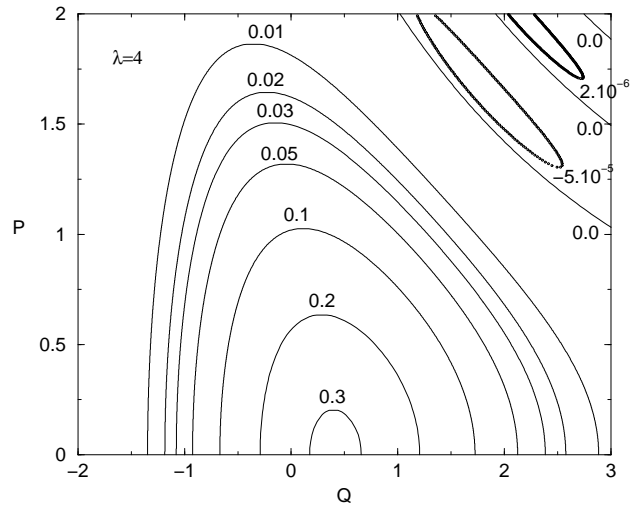


FIG. 7. Same as Fig. 5 for $\lambda = 4$.

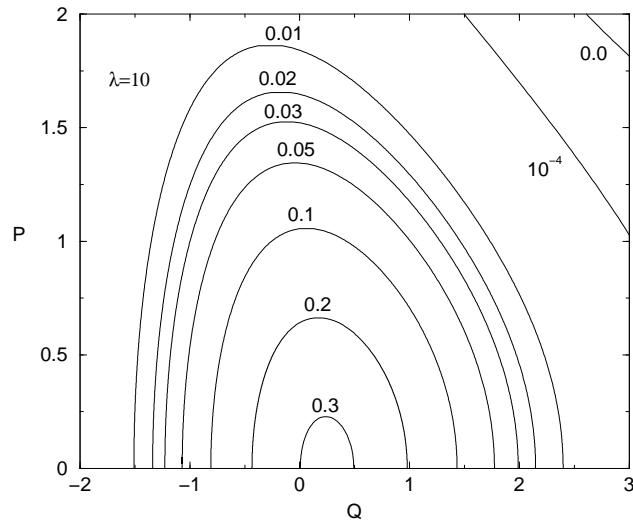


FIG. 8. Same as Fig. 5 for $\lambda = 10$.

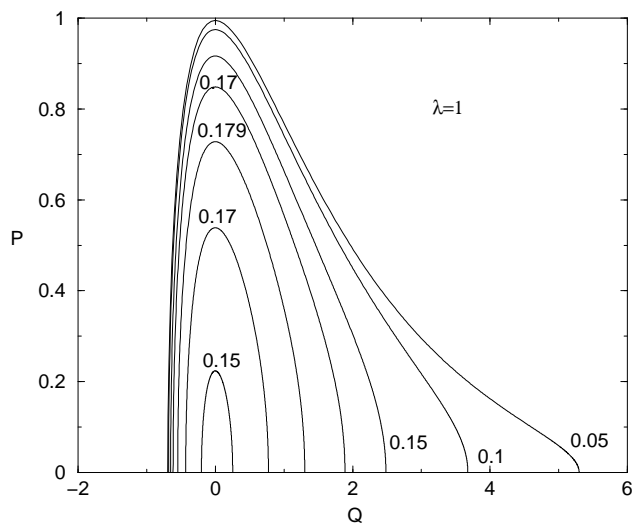


FIG. 9. Curves of constant semi-classical distribution function $\rho_c(Q, P)$ in units of \hbar^{-1} for the ground state of the Morse oscillator with $\lambda = 1$. For $0.145 < \rho_c < 0.179$ one has two curves for each value of ρ_c .

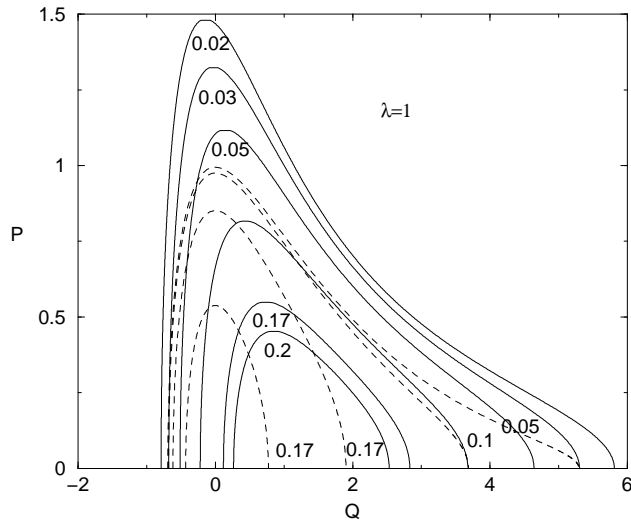


FIG. 10. Full curves are curves with a constant value of the Wigner distribution function ρ and dashed lines have constant value of the semiclassical distribution function ρ_c for the ground state of the Morse oscillator with $\lambda = 1$. Except for $\rho = 0.2$, for each full line with a given ρ one has one or two corresponding dashed lines with ρ_c such that $\rho_c = \rho$.

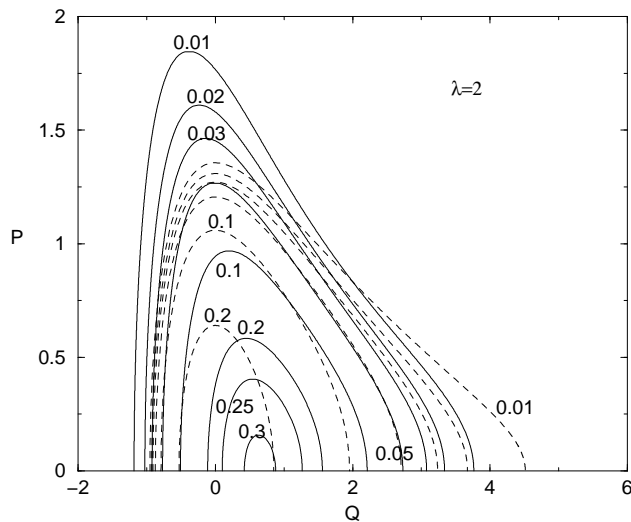


FIG. 11. Same as Fig. 10 for $\lambda = 2$. Except for $\rho = 0.3$ and $\rho = 0.25$, for each full line one has a corresponding dashed line with ρ_c such that $\rho_c = \rho$.

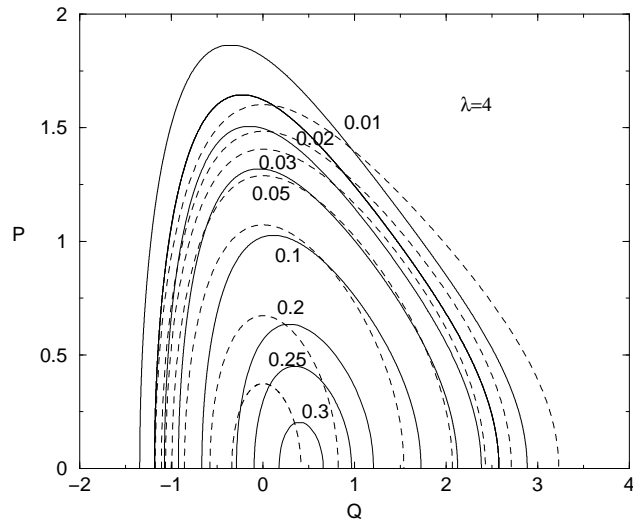


FIG. 12. Same as Fig. 10 for $\lambda = 4$. Except for $\rho = 0.3$, for each full line one has a corresponding dashed line with ρ_c such that $\rho_c = \rho$.

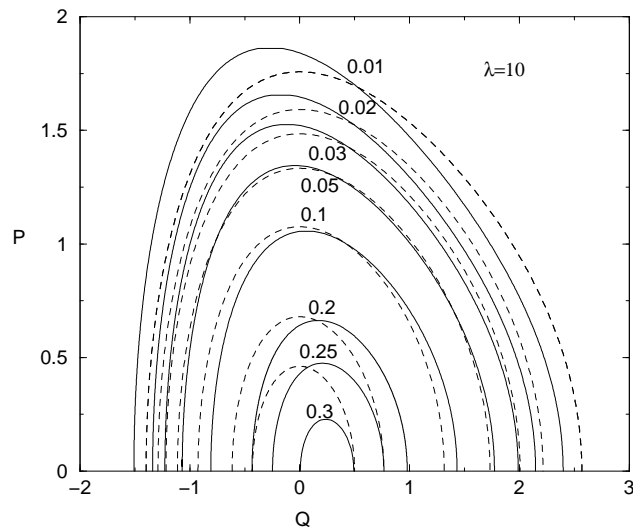


FIG. 13. Same as Fig. 10 for $\lambda = 10$. Except for $\rho = 0.3$, for each full line one has a corresponding dashed line with ρ_c such that $\rho_c = \rho$.